CCD Photometry, Light Curve Deconvolution, Period Analysis, and Evolutionary Status of the HADS Variable V417 Boötis

Kevin B. Alton
Desert Blooms Observatory, 70 Summit Avenue, Cedar Knolls, NJ 07927; kbalton@optonline.net

W. Allen Gilchrist, Jr.
Stonecrest Observatory, 104 Deer Ridge Drive, Fort Davis, TX 79734; gilchrist.allen@ymail.com

Received September 29, 2021; revised November 3, 2021; accepted December 1, 2021

Abstract CCD-derived photometric B- and V-magnitude data were acquired from V417 Boo, an intrinsic variable classically defined as a High Amplitude δ Scuti (HADS) star. Deconvolution of precise time-series light curve data was accomplished using discrete Fourier transformation and revealed a fundamental mode (f_0) of oscillation at ~11.5408 d^{-1} along with three other partial harmonics ($2f_0$–$4f_0$). No other statistically significant frequencies were resolved following successive pre-whitening of each residual signal. An assessment of potential period changes over time was performed using five new times of maximum (ToMx) light produced from the present study along with 34 other ToMx values mined from the AAVSO VSX archives. These results indicate that no substantive change in the fundamental period of oscillation or amplitude (V-mag) has likely occurred over the past 11 years. Finally, an investigation with PARSEC models for generating stellar tracks and isochrones provided valuable insight into the evolutionary status and physical nature of V417 Boo.

1. Introduction

Amongst the most common A- and F-type stars which exhibit variability are the multi-periodic δ Scuti-like (hereafter δ Sct) pulsating stars. These intrinsic variables occupy a narrow space at the intersection of the classical instability strip, pre-main sequence, and main sequence (MS) on the Hertzsprung-Russell diagram. Therein they represent a transition from the high-amplitude radial pulsators, such as Cepheid variables, and non-radial multi-periodic pulsators (Breger 2000). Main sequence δ Sct stars typically range from spectral type F2 to A2 (Rodríguez and Breger 2001) which correspond to effective temperatures varying between 6300 and 8600 K (Uytterhoeven *et al.* 2011). Hotter δ Sct stars generally have shorter pulsation periods (i.e. higher pulsation mode frequencies) than cooler δ Sct stars.

Pulsations in δ Sct stars are excited by the κ-mechanism operating in the He II partial ionization zone (T ~ 50000 K) which produce low-order pressure (p) modes akin to acoustic waves (Cox 1963; Chevalier 1971). These can produce radial pulsations which evoke symmetrical changes in stellar size and/or non-radial pulsations that give rise to asymmetric changes in shape but not volume. Although shorter periods (<30 min) have been observed (Holdsworth *et al.* 2014) in some A-type stars, the fundamental radial pulsations of Galactic δ Sct variables with near solar metallicity typically range between 0.05 to 0.25 d. Masses vary from ~ 1.2 $M_\odot$ to ~ 2.5 $M_\odot$, so they are more luminous and larger than our Sun.

The luminosity classes for δ Sct variables generally range from III (normal giants) to V (MS stars). δ Sct variables with moderate (40 km s^{-1}) to rapid (250 km s^{-1}) rotational velocities (v sin i) generally have small light curve amplitudes (ΔV ~ 0.01–0.03 mag) composed of a multitude of pulsation frequencies, most of them nonradial. Stars with slow rotational velocities (<30 km s^{-1}) tend to be radial pulsators and have light curve amplitudes (V-mag) in excess of 0.20–0.30 mag. The latter characteristics define a δ Sct subgroup called High-Amplitude δ Scuti stars (HADS).

Although HADS stars represent a very small fraction (<1%) of all δ Sct variables (Lee *et al.* 2008), they are attractive targets for the budding photometrist in possession of a modestly sized telescope and CCD camera. Given their comparatively short pulsation periods (<0.2 d), high modulation amplitude (>0.2 mag), and luminosity (>10 $L_\odot$) an entire light curve (LC) can be completed in just a few imaging sessions. HADS variables commonly oscillate via low-order single or double radial pulsation modes (Poretti 2003a, 2003b; Niu *et al.* 2013, 2017). A high percentage (~ 40%) are double pulsators showing simultaneous pulsations in the fundamental and the first overtone mode with amplitudes generally higher in the fundamental mode (McNamara 2000). It should be noted, however, that non-radial pulsations have also been detected with the HADS variable V974 Oph (Poretti 2003a, 2003b). HADS stars have historically been divided according to metallicity relative to our Sun ([Fe/H] = 0 dex). Members of the metal-poor ([Fe/H] << 0) group are called SX Phe stars, based on the eponymous prototype SX Phoenicis. Ostensibly they have shorter periods (0.02 < P < 0.125 d) and lower masses (~ 1.0–1.3 $M_\odot$) than their sibling HADS variables possessing near solar metal abundance. SX Phe stars frequently dwell in globular clusters (GC), ancient collections of Population II stars. Therein, the majority of SX Phe variables are classified as blue straggler stars, paradoxically appearing much younger than their GC cohorts. Despite previous claims to the contrary, Balona and Nemec (2012) make a strong case that it is not possible to differentiate between δ Sct and field SX Phe variables based on pulsation amplitude, the number of pulsation modes, period, or even metallicity (Garg *et al.* 2010). They further argue that the evolutionary status of each star is the only way to distinguish between these two classes. Much more sensitive space telescopes like NASA's Kepler (Gilliland *et al.* 2010; Guzik 2021; Yang *et al.* 2021), the European Space Agency's

CoRoT (Baglin 2003), the Canadian Microvariability and Oscillations of STars [MOST] (Walker *et al.* 2003), and the Transiting Exoplanet Survey Satellite, TESS (Ricker *et al.* 2015; Bedding *et al.* 2020) have detected a rich supply of HADS stars using highly precise photometry. New discoveries from Kepler and TESS have begun to blur the traditional line of distinction between HADS and SX Phe type variables.

An additional classification scheme for δ Scuti stars was recently proposed by Qian *et al.* (2018). Therein two distinct groups of δ Scuti stars were uncovered from the Large Sky Area Multi-Object Fiber Spectroscopic Telescope (LAMOST) survey (Zhao *et al.* 2012) that fundamentally differed in effective temperature. One group was identified as normal δ Scuti stars (NDSTs) when T_{eff} ranged between 6700–8500 K while the other was considered as unusual and cool variable stars (UCVs) with T_{eff} values less than 6700 K. A more restrictive fundamental pulsation range (0.09–0.22 d) coupled with being slightly metal-poor ([Fe/H] = –0.25–0.0) further differentiates the UCVs from the NDST group. Furthermore, once the UCV stars were excluded from consideration, empirically based temperature-period, log g-period, and metallicity-period relationships could be developed for NDSTs.

One of the most important astronomical events in history occurred when Henrietta Leavitt discovered a period-luminosity (P-L) relationship between 25 Cepheid variables in the Small Magellanic Cloud (Leavitt and Pickering 1912). Since then pulsating stars have served as standard candles for estimating cosmic distances to individual stars, clusters, and galaxies. Over time this P-L relationship has been refined owing to differences between metal-rich (Population~I) and metal-poor (Population II) Cepheids (Baade 1956).

A more modern refinement of the P-L relationship for δ Sct variables was reported by McNamara (2011), albeit with Hipparcos parallaxes and not the more accurate values determined by the Gaia Mission (Lindegren *et al.* 2016; Gaia Collab. *et al.* 2018). Nonetheless this empirically-derived expression (McNamara 2011) appears to correspond reasonably well to the main ridge of Gaia DR2 derived P-L relationship for δ Sct variables determined by Ziaali *et al.* (2019). The most recent investigation that resulted in the derivation of P-L relationships for δ Sct stars oscillating in the fundamental (adopted herein) as well as first through third overtones was reported by Poro *et al.* (2021).

The variability of V417 Boo (= NSVS 5189969) was first detected during the ROTSE-I survey between 1999 and 2000 (Akerlof *et al.* 2000; Woźniak *et al.* 2004). Accordingly, Hoffman *et al.* (2009) classified this star as a short period (P = 0.08665 d) δ Sct variable following an evaluation of unfiltered photometric data from the ROTSE-I Survey. Photometric (V-mag) data from V417 Boo (CSS J154137.0+515924) were also acquired during the Catalina Sky Survey (Drake *et al.* 2009) and the All-Sky Automated Survey for SuperNovae (ASAS-SN) (Shappee *et al.* 2014; Jayasinghe *et al.* 2021). Herein we report the first two-color photometric study on V417 Boo which uses discrete Fourier transformation to assess the fundamental pulsation modes along with secular analyses to establish whether there have been any obvious changes in magnitude and pulsation period.

2. Observations and data reduction

2.1. Photometry

Precise time-series images were acquired at Stonecrest Observatory (SO, USA: 103.9767 W, 30.6167 N) with an SBIG ST10-XME CCD camera installed at the secondary focus of a 0.3-m Ritchey Chretien telescope. This instrument produces an image scale of 1.15 arcsec/pixel (bin = 2 × 2) and a field of view (FOV) of 21' × 14'. Image acquisition (B: 120-s; V: 50-s) was performed using TheSkyX Pro Version 10.5.0 (Software Bisque 2019) which controlled an Astro-Physics AP-1200 GTO German equatorial mount. The CCD-camera was equipped with B and V filters manufactured to match the Johnson-Cousins Bessell specification. Dark subtraction, flat correction, and registration of all images collected at SO were performed with ImagesPlus Ver. 6.5 (Unsold 2000). Instrumental readings were reduced to catalog-based magnitudes using the APASS star fields (Henden *et al.* 2009, 2010, 2011; Smith *et al.* 2011) built into MPO Canopus v10.8.5.0 (Minor Planet Observer 2010). LCs for V417 Boo were generated using an ensemble of five non-varying comparison stars. The identity, J2000 coordinates, and APASS color indices (B–V) for these stars are provided in Table 1; a corresponding FOV image is rendered in Figure 1. Only data from images taken above 30° altitude (airmass <2.0) were included; considering the proximity of all program stars, differential atmospheric extinction was ignored. During each imaging session comparison stars typically stayed within ± 0.009 mag for both passbands.

3. Results and discussion

3.1. Photometry and ephemerides

Photometric values in B (n = 231) and V (n = 249) passbands were separately processed to produce LCs acquired between 28 April (JD 2459332.71243) and 26 May 2021 (JD 2459360.90958) (Figure 2). Period determinations were initially performed using Peranso v2.5 (Vanmunster 2011) by applying periodic orthogonals (Schwarzenberg-Czerny 1996) to fit observations and analysis of variance (ANOVA) to assess fit quality. In this case a similar period solution for each passband (0.086649 ± 0.000002 d) was obtained. Separately folding the sparsely sampled CSS and ASAS-SN survey data with those (V-mag) acquired at SO yielded a period at 0.086648 ± 0.000008 d and 0.086649 ± 0.000002 d, respectively (Figure 3). New ToMx light values were estimated using the polynomial extremum fit utility featured in Peranso (Paunzen and Vanmunster 2016). There was no obvious color dependency on the SO timings such as those reported for other δ Sct variables (Elst 1978); therefore, corresponding B and V data were averaged (Table 2) at each time of maximum (ToMx). New maxima from SO (5) along with published results starting in 2010 (Table 2) and values (34) derived from the AAVSO International Variable Star Index (VSX; Watson *et al.* 2014) archive were used to establish whether there were any pulse timing differences (PTD) between the observed and predicted fundamental period of oscillation. The reference epoch (15 April 2020, VSX) was initially defined by the following linear ephemeris (Equation 1):

Table 1. Astrometric coordinates (J2000), V-magnitude and color indices (B–V) for V417 Boo and five comparison stars (1–5) used during this photometric study.

FOV Identification	*Star Identification*	*R. A. (J2000) h m s*	*Dec. (J2000) deg ′ ″*	*APASSa V-mag.*	*APASSa (B-V)*
T	V417 Boo	15 41 36.994	+51 59 24.99	13.017	0.324
1	GSC 03489-00958	15 41 12.732	+52 02 29.66	11.832	0.843
2	GSC 03489-00854	15 41 46.077	+52 03 48.99	12.302	0.731
3	GSC 03489-01407	15 42 03.317	+52 02 55.97	11.045	1.193
4	GSC 03489-01132	15 42 27.265	+52 03 50.33	11.635	0.841
5	GSC 03489-01298	15 41 34.504	+51 56 00.86	14.175	0.775

a. V-magnitude and (B–V) for comparison stars derived from APASS database described by Henden et al. *(2009, 2010, 2011) and Smith* et al. *(2010), as well as on the AAVSO web site (https://www.aavso.org/apass).*

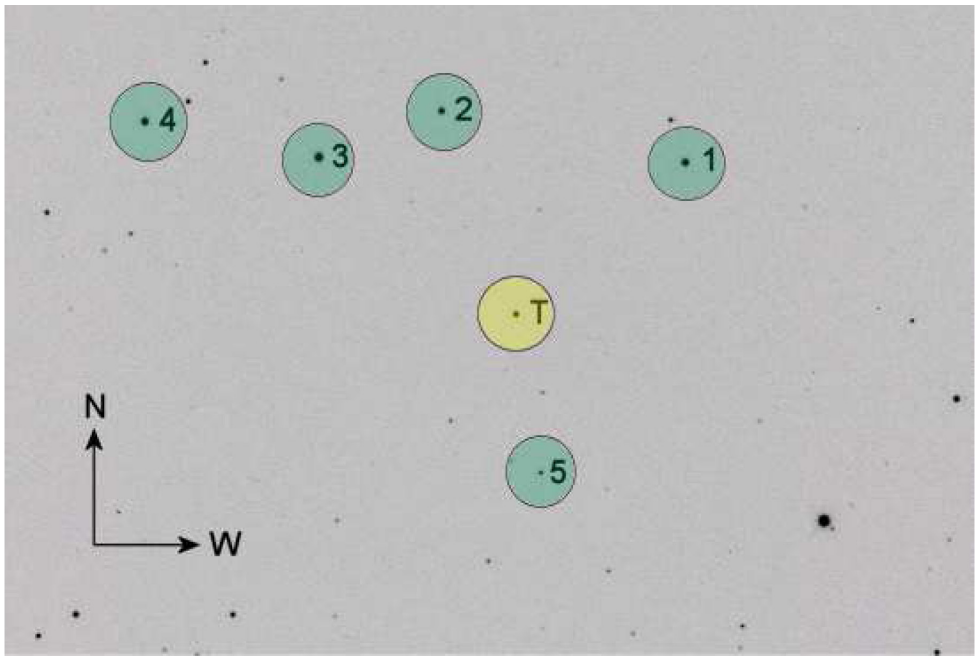

Figure 1. V417 Boo (T) along with the five comparison stars (1–5) used to reduce time-series images to APASS-catalog based magnitudes.

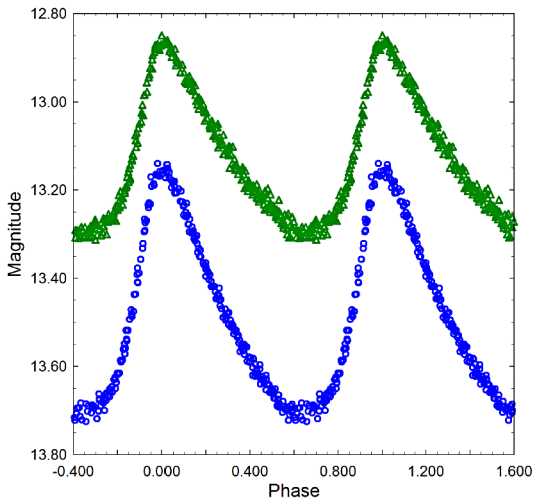

Figure 2. Period folded (0.086640 d) LCs for V417 Boo produced from photometric data obtained between 28 April and 26 May 2021 at SO. LCs shown at the top (V) and bottom (B) represent catalog-based (APASS) magnitudes determined using MPO Canopus.

$$\text{Max (HJD)} = 2458955.406 + 0.08664937\ E. \quad (1)$$

As shown in Figure 4, secular changes in pulsation period can potentially be uncovered by plotting the PTD residuals vs. epoch (or cycle number). Thus far, this relationship is basically described by a straight line and suggests that little or no change to the period has occurred since 2010. The updated ephemeris (Equation 2) based on maximum light timing data available through May 2021 is as follows:

$$\text{Max (HJD)} = 2459360.83902\ (9) + 0.08664937\ (1)\ E, \quad (2)$$

where the times of maxima are in Heliocentric Julian Dates (HJD), and E is an integral cycle number chosen so that E = 0 represents the most recent maximum measurement.

These results, along with nearly superimposable period-folded LCs from SO, CSS, and ASAS-SN (Figure 3), further support that the fundamental pulsation period has not substantively changed since 2010 nor has the V-mag amplitude changed significantly over the same period of time.

Table 2. Differences between the times-of-maximum light (HJD) predicted from the updated linear ephemeris (Equation 2) and those observed for V417 Boo between 2010 and 2021.

HJD 2400000+	Epoch (Cycle No.)	PTD[a]	Reference[b]	HJD 2400000+	Epoch (Cycle No.)	PTD[a]	Reference[b]
55334.4160	–46468	–0.00023	1	58474.6756	–10227	–0.00039	6
55334.5016	–46467	–0.00128	1	58523.6323	–9662	–0.00052	6
55713.3338	–42095	–0.00011	2	58523.7193	–9661	–0.00019	6
55713.4204	–42094	–0.00016	2	58654.5594	–8151	–0.00068	6
55729.3637	–41910	–0.00035	2	58694.4190	–7691	0.00023	6
55729.4504	–41909	–0.00030	2	58715.3880	–7449	0.00007	6
55729.5369	–41908	–0.00045	2	58747.3613	–7080	–0.00022	6
56075.4428	–37916	0.00118	3	58917.5421	–5116	0.00127	6
56075.5293	–37915	0.00103	3	58950.3813	–4737	0.00029	6
56349.8601	–34749	–0.00007	4	58950.5537	–4735	–0.00055	6
56349.9467	–34748	–0.00011	4	58955.4073	–4679	0.00067	6
56385.3868	–34339	0.00039	4	58958.6992	–4641	–0.00013	6
56385.4731	–34338	0.00004	4	58958.6994	–4641	0.00005	6
56730.5108	–30356	–0.00004	5	58958.7855	–4640	–0.00042	6
56730.5976	–30355	0.00012	5	58958.7857	–4640	–0.00023	6
56730.6841	–30354	–0.00003	5	58968.7509	–4525	0.00026	6
56793.5048	–29629	–0.00013	5	59270.6370	–1041	–0.00008	6
56793.5918	–29628	0.00023	5	59302.5245	–673	0.00050	6
57071.4758	–26421	–0.00028	6	59302.6101	–672	–0.00054	6
57071.5630	–26420	0.00027	6	59327.4792	–385	0.00016	6
57514.4277	–21309	–0.00001	6	59332.7644	–324	–0.00026	7
57803.5761	–17972	–0.00049	6	59334.4114	–305	0.00041	6
57803.6627	–17971	–0.00060	6	59339.6967	–244	0.00007	7
57828.5314	–17684	–0.00019	6	59342.3830	–213	0.00028	6
57828.6177	–17683	–0.00052	6	59342.4696	–212	0.00021	6
58173.6559	–13701	–0.00013	6	59344.7227	–186	0.00043	7
58246.3552	–12862	0.00036	6	59353.9069	–80	–0.00014	7
58246.4411	–12861	–0.00037	6	59360.8389	0	–0.00017	7
58247.4816	–12849	0.00024	6				

a. PTD = Time difference between observed fundamental pulsation time–of–maximum and that calculated using the reference ephemeris (Equation 2).
b. 1. Wils et al. *(2011); 2. Wils* et al. *(2012); 3. Wils* et al. *(2013); 4. Wils* et al. *(2014); 5. Wils* et al. *(2015); 6. AAVSO–VSX (Watson* et al. *2014); 7. This study.*

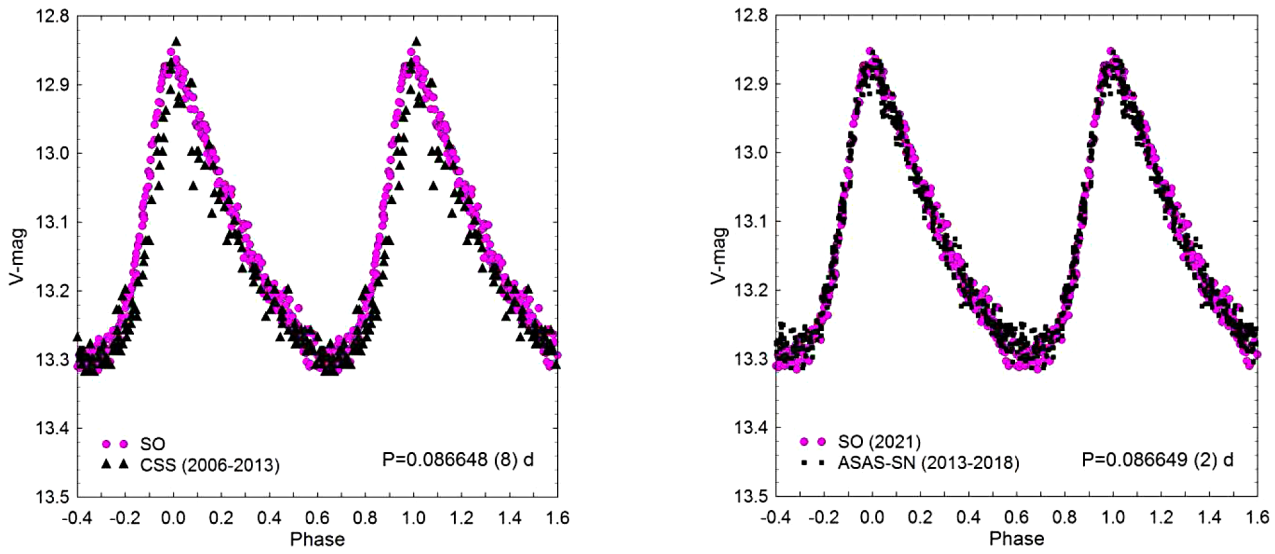

Figure 3. Period-folded LCs for V417 Boo produced from precise photometric V-magnitude data obtained at SO (2021) along with sparsely sampled data from the CSS (2006–2013) and ASAS-SN (2013–2018) surveys. CSS and ASAS-SN magnitudes were offset to conform with the APASS-derived values from SO.

Table 3. Fundamental frequency (f_0) and corresponding partial harmonics ($2f_0$–$4f_0$) detected following DFT analysis of time-series photometric data (B and V) from V417 Boo.

	Frequency (d^{-1})	*Frequency Error*	*Amplitude (mag)*	*Amplitude Error*	*Phase*	*Phase Error*	*S/N*
f_0-B	11.54078	0.00009	0.24961	0.00121	0.66076	0.00066	140.7
f_0-V	11.54084	0.00009	0.19006	0.00110	0.94685	0.30980	103.8
$2f_0$-B	23.08167	0.00030	0.07345	0.00149	0.60829	0.00273	59.6
$2f_0$-V	23.08168	0.00030	0.05988	0.00106	0.03210	0.28679	37.6
$3f_0$-B	34.62231	0.00077	0.02968	0.00159	0.17567	0.00783	20.4
$3f_0$-V	34.62314	0.00079	0.02260	0.00114	0.89959	0.32002	17.8
$4f_0$-B	46.16234	0.03573	0.01290	0.00238	0.55778	0.10054	8.2
$4f_0$-V	46.16235	0.00125	0.01350	0.00113	0.08956	0.31381	8.8

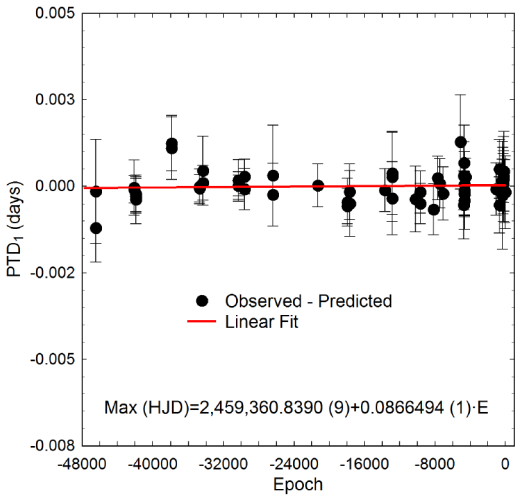

Figure 4. Straight line fit (PTD vs. epoch) suggesting that little or no change to the fundamental mode of oscillation for V417 Boo had occurred between 2010 and 2021.

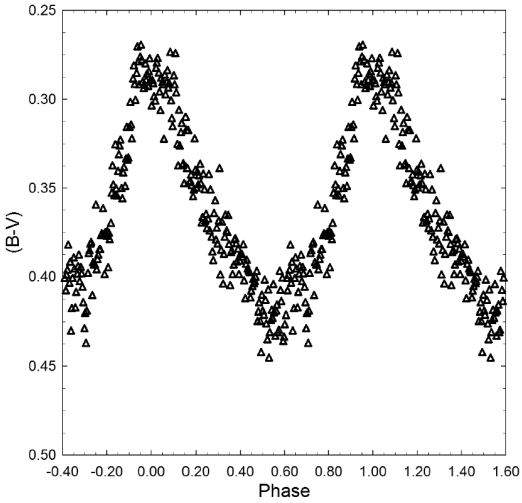

Figure 5. V417 Boo LCs illustrating significant change in color index ($0.28 < (B–V) < 0.41$) as maximum light slowly descends to minimum light. This effect is most closely associated with a decrease in the effective surface temperature during minimum light.

3.2. Light curve behavior

Characteristically, light curves from HADS variables are asymmetrical with a faster ascent from minimum to maximum light than the decline back to minimum brightness. V417 Boo appears to be a textbook example in this regard (Figure 2). The largest difference between maximum and minimum light is observed in the blue passband (ΔB-mag = 0.55), followed by V (ΔV-mag = 0.47). This behavior is typical for pulsating F- to A-type stars. It follows when the B- and V-mag LCs are binned into equal phase intervals and then subtracted from one another, the emerging LC (B–V) exhibits significant reddening during minimum light (Figure 5). In this case color excess (B–V) ranges between 0.28 and 0.41 mag. Estimates for interstellar extinction (A_V) vary widely depending on the model selected (Amôres and Lépine 2005, 2007; Schlegel *et al.* 1998; Schlafly and Finkbeiner 2011). Access to these data is greatly facilitated via the GALextin website at http://www.galextin.org/. The median reddening value ($E(B–V) = 0.0361 \pm 0.0119$ mag) corresponds to an intrinsic color index $(B–V)_0$ for V417 Boo that varies between 0.191 ± 0.028 at maximum light and 0.372 ± 0.032 mag at minimum brightness. Based on the corrected (Torres 2010) polynomial transformation equations derived by Flower (1996), the mean effective temperature (T_{eff}) was estimated to be 7310 ± 223 K, with a minimum T_{eff} of $\sim 6859 \pm 151$ K and a maximum T_{eff} of $\sim 7814 \pm 171$ K. These results based strictly on B–V photometry at SO are in good agreement with the Johnson-Cousins transformations (Warner 2007) from 2MASS (Skrutskie *et al.* 2006). When transformed, J- and K-band data from 2MASS predict a T_{eff} value of 7673 ± 315 K. A low resolution UV-vis spectrum has been reported by LAMOST DR5 (Zhao *et al.* 2012; Wang *et al.* 2019) that is consistent with an A7V classification for V417 Boo ($T_{eff} = 7608 \pm 54$ K). We adopted the median value (7640 ± 181 K) derived from our LCs, 2MASS, LAMOST DR5, and Gaia DR2. According to Qian *et al.* (2018), V417 Boo would be considered a NDST rather than a UCV since T_{eff} is between 6700 and 8500 K, while the fundamental pulsation period is less than 0.09 d.

3.3. Light curve analysis by discrete Fourier transformation

LC deconvolution was performed with Period04 (Lenz and Breger 2005) wherein discrete Fourier transformation (DFT) was used to extract the fundamental pulsating frequency (spectral window = 100 d^{-1}). Pre-whitening steps which successively remove the previous most intense signals were employed to tease out other potential oscillations from the residuals. Only those frequencies with a $S/N \geq 6$ (Baran *et al.* 2014) in each passband are presented in Table 3. In all cases, uncertainties in frequency, amplitude, and phase were estimated by the Monte Carlo simulation (n = 400) routine built into Period04.

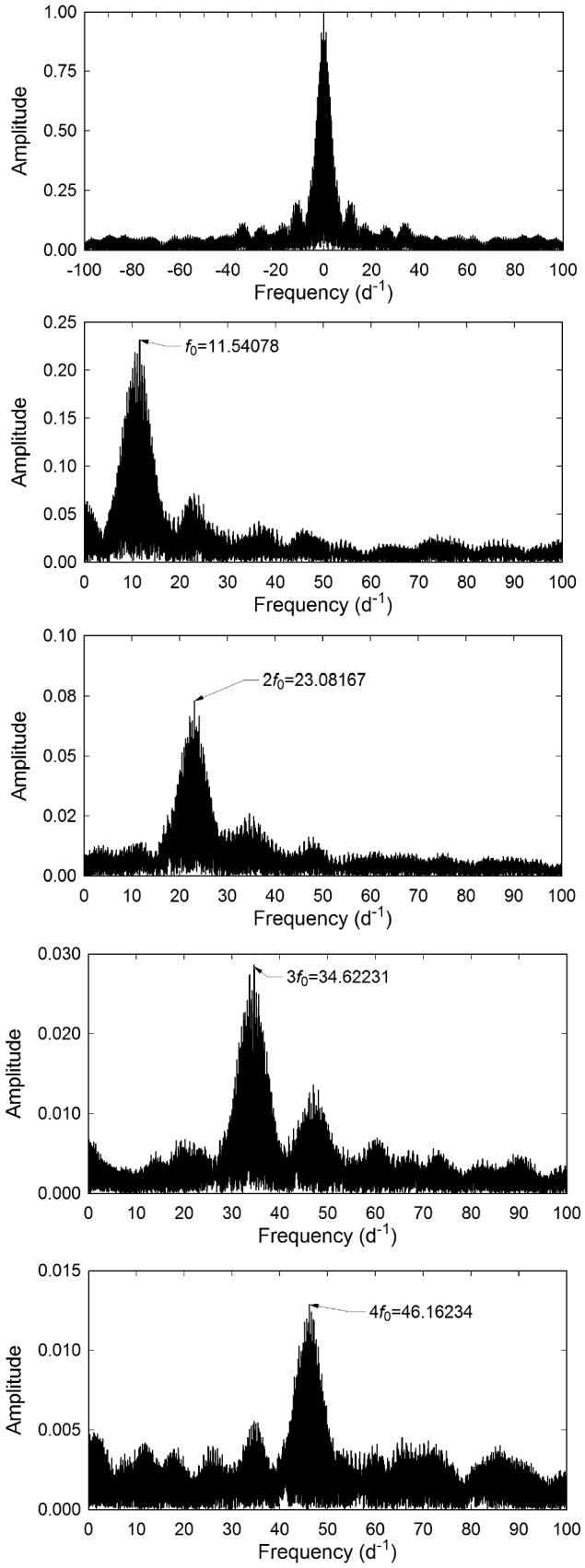

Figure 6. B-magnitude spectral window (top) and all significant pulsation frequencies following DFT analysis of photometric data from V417 Boo acquired in 2021 at SO. The amplitude spectra illustrate the fundamental (f_0) frequency and its highest partial harmonic ($4f_0$) which was clearly detected (S/N ≥ 8) following prewhitening.

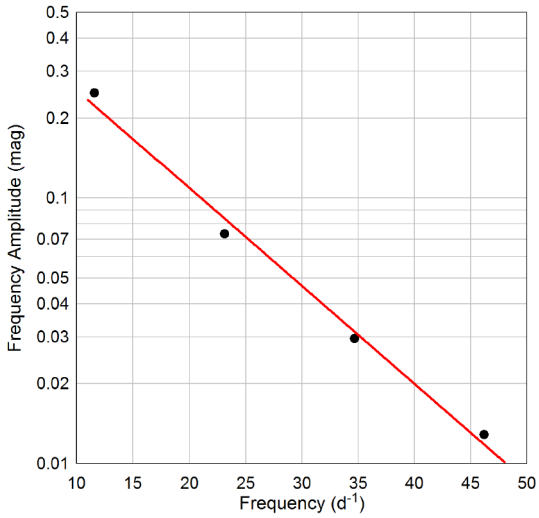

Figure 7. Amplitude decay of the fundamental (f_0) pulsation period and its corresponding partial harmonics ($2f_0$–$4f_0$) observed in the B-passband.

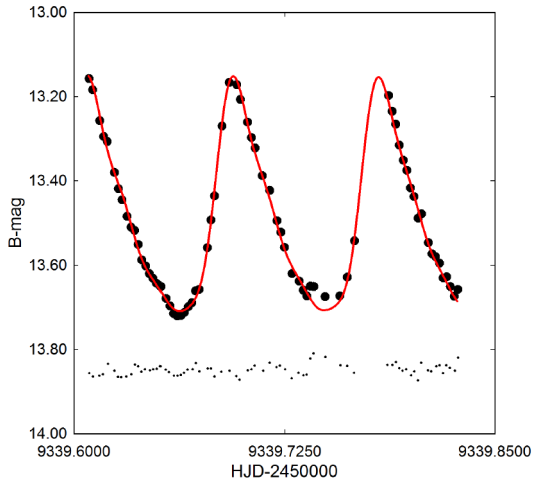

Figure 8. Representative fit of B-mag time-series data (05 May 2021) based on elements derived from DFT. Model fit residuals at bottom are offset by constant amount to compress y-axis scale.

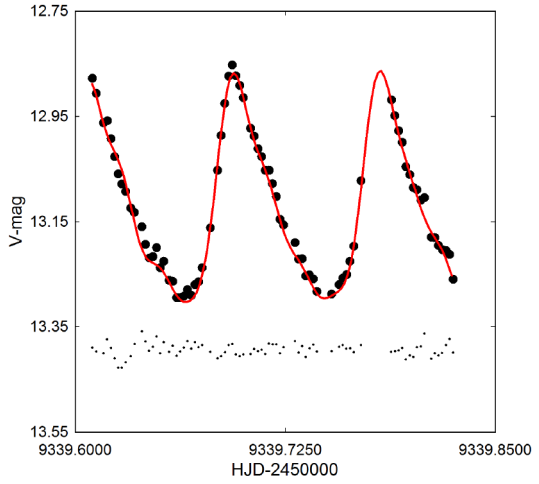

Figure 9. Representative fit of V-magitude time-series data (05 May 2021) based on elements derived from DFT. Model fit residuals at bottom are offset by constant amount to compress y-axis scale.

Our results strongly suggest that V417 Boo is a monoperiodic radial pulsator; changes in stellar size during each pulsation cycle are therefore symmetrical. The spectral window and amplitude spectra derived from the B-passband data are illustrated in Figure 6; others from V-passband are not included since they are essentially redundant with respect to detected frequencies. As would be expected, the fundamental pulsation period ($f_0 \simeq 11.5408\,d^{-1}$ has the greatest amplitude. Successive pre-whitening steps uncovered statistically significant partial harmonics out as far as $4f_0$. The amplitude decay appears to be exponential as a function of harmonic order (Figure 7), a behavior that has been observed with other HADS variables such as VX Hya (Templeton *et al.* 2009) and RR Gem (Jurcsik *et al.* 2005). Although no other independent pulsation modes were detected during this short campaign, it is acknowledged that a longer baseline in time from multiple sites would be required to validate this claim (Breger 2000). Representative LC fits to B- and V-mag time-series data (05 May 2021) following DFT analysis are respectively illustrated in Figures 8 and 9.

3.4. Global parameters

Absolute visual magnitude (M_V) was estimated (1.800 ± 0.015) after substituting the pulsation period (P = 0.08664937 d) into Equation 3, the P-L relationship reported by Poro *et al.* (2021) for δ Scuti stars oscillating in a fundamental radial mode:

$$M_V = (-3.200 \pm 0.010) \log (P) - (1.599 \pm 0.010). \quad (3)$$

Thereafter applying known values for m, ($V_{avg} = 13.112 \pm 0.031$), $A_V = 0.1119 \pm 0.0370$), and M_V, the reddening-corrected distance modulus (Equation 4):

$$d(pc) = 10^{(m - M_V - A_V + 5)/5)}, \quad (4)$$

produced an estimated distance (1737 ± 40 pc) to V417 Boo. This value is within 4.5% of the Gaia DR2 determination of distance ($1663^{+79.2}_{-72.4}$ pc) calculated from parallax using the Bailer-Jones bias correction (Bailer-Jones 2015). As it turns out V417 Boo is in a region of the Milky Way (Gal. coord. (J2000): l = 82.8255; b = 49.7338) where corrections for interstellar extinction ($A_V = 0.1119$) should be included. This is an important distinction when comparing our results to those reported in Gaia DR2 wherein interstellar extinction (A_G) is assumed to be zero. Accordingly the luminosity and radius were determined (Table 4) as follows where $V_{avg} = 13.112 \pm 0.031$, $A_V = 0.1119 \pm 0.037$, $M_V = 1.783$, and $BC_V = 0.0312$. Luminosity ($L_* = 14.52 \pm 0.20\,L_\odot$) was calculated according to Equation 5:

$$\frac{L_*}{L_\odot} = 10^{((M_{bol\odot} - M_{bol*})/2.5)}, \quad (5)$$

where $M_{bol\odot} = 4.74$ and $M_{bol*} = 1.835$. Finally, the radius of V417 Boo in solar units ($R_* = 2.18 \pm 0.02$) was estimated using the well-known relationship (Equation 6) where:

$$\frac{L_*}{L_\odot} = \left(\frac{R_*}{R_\odot}\right)^2 \left(\frac{T_*}{T_\odot}\right)^4. \quad (6)$$

Table 4. Global stellar parameters for V417 Boo using empirically derived values and those predicted from the PARSEC model where Z = 0.020.

Parameter	*SO*	*PARSEC*
Mean T_{eff} [K]	7640 ± 181	7640 ± 181
Luminosity [$L_\odot$]	14.52 ± 0.20	14.52 ± 0.20
Mass [$M_\odot$]	1.87 ± 0.01	1.82 ± 0.02
Radius [$R_\odot$]	2.18 ± 0.02	2.21 ± 0.01
rho [g/cm3]	0.256 ± 0.006	0.238 ± 0.003
log g [cgs]	4.034 ± 0.042	4.010 ± 0.012
Q [d]	0.037 ± 0.002	0.036 ± 0.001

Stellar radius was independently estimated from an empirically derived period-radius (P-R) relationship (Equation 7) reported by Laney *et al.* (2003) for HADS stars and classical Cepheids:

$$\log(R_*) = a + b \cdot \log(P) + c, \quad (7)$$

where $a = 1.106 \pm 0.012$, $b = 0.725 \pm 0.010$, and $c = 0.029 \pm 0.024$. In this case the value for R_* ($2.32 \pm 0.36\,R_\odot$) was 13.8% higher than value obtained from observations at SO ($2.18 \pm 0.02\,R_\odot$).

Unlike the mass derived from the Keplerian motion of binary stars, the mass of a single isolated field star is very difficult to determine accurately. We adopted a model using MS stars in detached binary systems (Eker *et al.* 2018) which established a mass-luminosity relationship ($1.05 < M/M_\odot \leq 2.40$) according to the following equation:

$$\log(L) = 4.329(\pm 0.087) \cdot \log(M) - 0.010(\pm 0.019), \quad (8)$$

whereby a mass value in solar units ($1.865 \pm 0.014\,M_\odot$) was calculated. Other derived values for density ($\rho_\odot$), surface gravity (log g), and pulsation constant (Q) are also included in Table 4 along with those estimated from evolutionary modeling (section 3.5). Stellar density (ρ_*) in solar units (g/cm^3) was calculated according to Equation 9:

$$\rho_* = \frac{3 \cdot G \cdot M_* \cdot m_\odot}{4\pi (R_* \cdot r_\odot)^3}. \quad (9)$$

where G = the gravitational constant ($6.67408 \cdot 10^{-8}\,cm \cdot g^{-1} \cdot sec^{-2}$), $m_\odot$ = solar mass (g), $r_\odot$ = solar radius (cm), M_* is the mass, and R_* the radius of V417 Boo in solar units. Using the same algebraic assignments, surface gravity (log g) was determined by the following expression:

$$\log g = \log \left(\frac{M_* \cdot m_\odot \cdot G}{(R_* \cdot r_\odot)^2}\right). \quad (10)$$

When attempting to characterize p-mode pulsations (radial) it is helpful to introduce the concept of a pulsation constant (Q). The dynamical time that it takes a p-mode acoustic wave to internally traverse a star is related to its size but more accurately the mean density. This is defined by the period-density relationship:

$$Q = P \sqrt{\bar{\rho}_* / \bar{\rho}_\odot}. \quad (11)$$

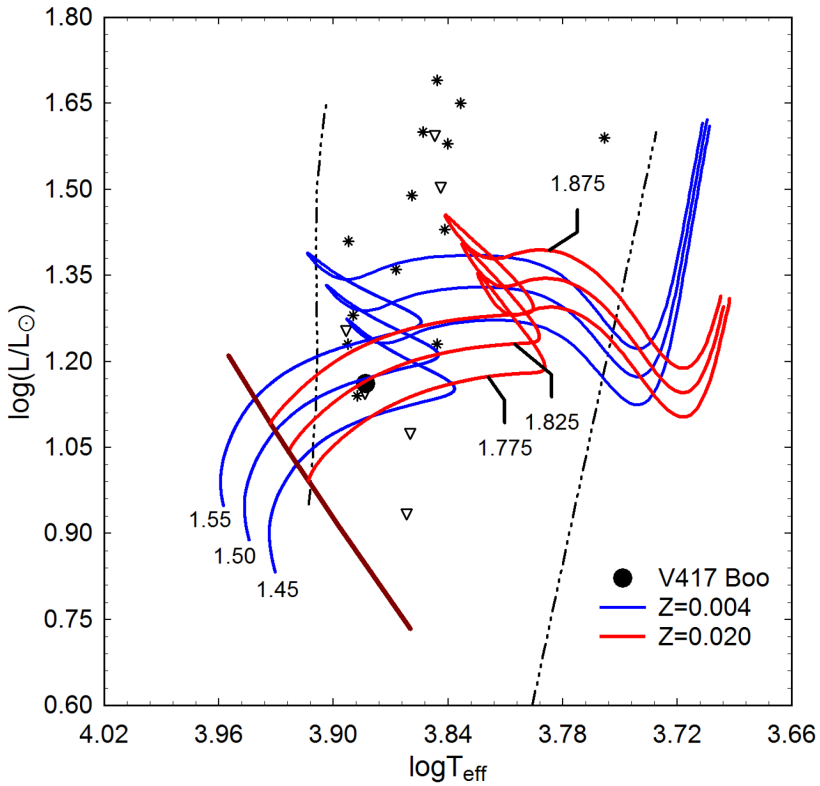

Figure 10. Evolutionary tracks (red solid line: Z = 0.020 at 1.775, 1.825, and 1.875 $M_\odot$ and blue line: Z = 0.004 at 1.45, 1.50, and 1.55 $M_\odot$) derived from PARSEC models (Bressan *et al.* 2012). The position of V417 Boo (●) is shown relative to ZAMS (thick maroon line) and within the theoretical instability strip (dashed lines) for radial low-p mode pulsators. Asterisks denote the positions of known HADS stars while open triangles (▽) indicate the position of SX Phe stars (Balona 2018).

where P is the pulsation period (d) and $\bar{\rho}_*$ and $\bar{\rho}_\odot$ are the mean densities of the target star and Sun, respectively. The mean density of an isolated field star like V417 Boo can not be determined without great difficulty. However, it can be expressed in terms (Equation 12) of other measurable stellar parameters where:

$$\log(Q) = -6.545 + \log(P) + 0.5\log(g) + 0.1M_{bol} + \log(T_{eff}). \quad (12)$$

The full derivation of this expression is provided by Breger (1990). The resulting Q values (Table 4) derived from observations at SO are consistent with theory (Q = 0.032 d) and the distribution of Q-values (0.03–0.04 d) from fundamental radial pulsations observed with other δ Sct variables (Breger 1979; Joshi and Joshi 2015; Antonello and Pastori 1981).

Finally, we attempted to get a comparative sense of how the physical size, temperature, and brightness of V417 Boo changes over the course of a single 2.08-hour pulsation. As shown in Figure 5 there is a significant change in color index (B–V) as maximum light descends to minimum light. Intrinsic color reveals that at maximum light, where $(B-V)_0 = 0.192 \pm 0.028$, the corresponding effective temperature is 7814 ± 171 K, whereas at minimum light ($(B-V)_0 = 0.372 \pm 0.032$) the estimated effective temperature is 6859 ± 151 K. Between these two extremes the putative rise in temperature (+956 K) would correspond to a 1.4-fold increase in luminosity with a relatively small decrease (9.4%) in radius. This rather crude estimate for changes in stellar radius would be best performed using the Baade-Wesselink method developed by Wesselink (1946), should radial velocity data over an entire oscillation cycle become available for this system.

3.5. Evolutionary status of V417 Boo

We can attempt to describe the evolutionary status of this variable using our estimates for luminosity and effective temperature. These values are plotted in the theoretical Hertzsprung-Russell diagram (HRD) shown in Figure 10. Here, the thick solid line gives the Zero Age Main Sequence (ZAMS) position for stars with solar metallicity (Z = 0.020) while two broken lines nearly perpendicular to the ZAMS delimit the blue and red edges of the theoretical instability strip for radial low-p modes (Xiong *et al.* 2016). The positions of several known (Balona 2018) δ Scuti (*) and SX Phe types (▽) are marked. The solid black circle indicates the position of V417 Boo using the SO-derived parameters and corresponding error estimates provided in Table 4. To determine the mass and age of V417 Boo from theoretical evolutionary tracks, its metallicity, Z, the total amount of metals by mass, needs to be known. Unfortunately, a high resolution spectrum is not available for this star so no direct measurement of Z exists. Nonetheless, we can try to estimate its value indirectly. A useful calculation:

$$z = d \cdot \sin(b), \quad (13)$$

where d is distance in pc (1663) and b is the Galactic latitude (49.7338°) places V417 Boo nearly 1267 pc above the Galactic plane in thick disk territory and not the halo, an area generally occupied by older metal-poor stars. We can therefore assume that V417 Boo approaches solar metallicity, or at most a few times lower, which also corresponds to the metallicity of metal-rich globular clusters classified as Oosterhoff type I.

A definitive measure for total solar metallicity, Z, remains elusive despite the fact that the Sun is our closest star. Values obtained over the last few decades range between 0.012 and 0.020, including one derived by Asplund *et al.* (2009) where $Z_{\odot} = 0.0142$. However, von Steiger and Zurbuchen (2016) challenged this result after obtaining a value of $Z_{\odot} = 0.0196 \pm 0.0014$ based on the chemical composition of solar wind. Soon thereafter, Serenelli *et al.* (2016) showed that their analysis of the solar wind was in serious disagreement with observables from the basic solar model so it cannot be representative of the solar interior. Obviously, a precise value for $Z_{\odot}$ still remains an open question (Vagnozzi 2019). Nonetheless, we plot two series of PARSEC evolutionary models (Bressan *et al.* 2012) in Figure 10 wherein red solid lines show the models with $Z = 0.020$ and blue solid lines define the models with $Z = 0.004$. The latter models would correspond to a decrease in metallicity by a factor of 3 to 5, depending on the reference solar metallicity. Assuming $Z = 0.020$, it can be shown by linear interpolation from the closest isochrone ($1.825 M_{\odot}$) that V417 Boo has a mass of $1.82 \pm 0.02\ M_{\odot}$. As depicted in Figure 10, the isochrone defined by a MS star with mass $1.825\ M_{\odot}$ ranges in age from $1.01 \cdot 10^8$ to $1.64 \cdot 10^9$ yr, wherein V417 Boo falls at 0.95 ± 0.10 Gyr. Each isochrone model contains predictions about changes in T_{eff}, $L_{\odot}$, and $R_{\odot}$ with time. The observed luminosity and effective temperature of V417 Boo lies within a range of predicted values where $R_{\odot} = 2.21 \pm 0.01$. Alternatively, a metal-poor ($Z = 0.004$) star would likely be somewhat smaller ($R_{\odot} = 2.15 \pm 0.03$), less massive ($M_{\odot} = 1.51 \pm 0.07$), and older ($1.71 \pm 0.01$ Gyr). V417 Boo lies well within the instability strip among the other known HADS stars. Uncertainty in the determination of mass will hopefully improve should high resolution spectroscopic data become available for V417 Boo in the future.

4. Conclusions

This first two-color (B and V) CCD study of V417 Boo has produced 39 new times of maximum which, along with other published values, lead to an updated linear ephemeris. Potential changes in the pulsation period assessed using the observed and predicted times of maximum suggest that since 2010 no significant change has occurred. Deconvolution of time-series photometric data by discrete Fourier transformation indicates that V417 Boo is a monoperiodic radial pulsator ($f_0 \simeq 11.5408\ d^{-1}$) which also oscillates in at least three other partial harmonics ($2f_0$–$4f_0$). A low resolution spectrum suggested an A7V classification, which was consistent with the adopted median effective temperature (7640 ± 181 K). These results, along with the distance estimate (1737 ± 40 pc), agreed reasonably well with the same findings (1663^{-72}_{+79} pc) provided by Gaia DR2. The pulsation period (0.0866494 d), oscillation mode (radial), V_{mag} amplitude (0.45 mag), and LC morphology are all consistent with the defining characteristics of a HADS variable. Furthermore, evolutionary tracks from the PARSEC model which assume near solar abundance ($Z = 0.020$) for V417 Boo are best matched by a MS star with a mass of $1.82 \pm 0.02\ M_{\odot}$ and radius of $2.21\ R_{\odot}$. These results are consistent with an independent mass estimate, $1.87 \pm 0.01\ M_{\odot}$, derived from an empirical mass-luminosity relationship (Eker *et al.* 2018). It would appear that the estimated mass of V417 Boo (1.80–$1.90\ M_{\odot}$) exceeds the generally accepted threshold ($M < 1.3\ M_{\odot}$) for SX Phe stars (McNamara 2011).

5. Acknowledgements

This research has made use of the SIMBAD database operated at Centre de Données astronomiques de Strasbourg, France. Time of maximum light data from the *Information Bulletin on Variable Stars* (IBVS) website (https://konkoly.hu/IBVS/IBVS.html) proved invaluable to the assessment of potential period changes experienced by this variable star. In addition, the International Variable Star Index maintained by the AAVSO, the All-Sky Automated Survey for Supernovae, and the Catalina Sky Survey (CSDR1) maintained at CalTech were mined for critical information. This work also presents results from the European Space Agency (ESA) space mission Gaia. Gaia data are being processed by the Gaia Data Processing and Analysis Consortium (DPAC). Funding for the DPAC is provided by national institutions, in particular the institutions participating in the Gaia MultiLateral Agreement (MLA). The Gaia mission website is https://www.cosmos.esa.int/gaia. The Gaia archive website is https://archives.esac.esa.int/gaia. The use of public data from LAMOST is also acknowledged. Guoshoujing Telescope (the Large Sky Area Multi-Object Fiber Spectroscopic Telescope LAMOST) is a National Major Scientific Project built by the Chinese Academy of Sciences. Funding for the project has been provided by the National Development and Reform Commission. LAMOST is operated and managed by the National Astronomical Observatories, Chinese Academy of Sciences. The diligence and dedication shown by all associated with these organizations is very much appreciated. We gratefully acknowledge the careful review and helpful commentary provided by an anonymous referee and Editor Morrison.

References

Akerlof, C., *et al.* 2000, *Astron. J.*, **119**, 1901.
Amôres, E. B. and Lépine, J. R. D. 2005, *Astron. J.*, **130**, 659.
Amôres, E. B. and Lépine, J. R. D. 2007, Astron. J., 133, 1519.
Antonello, E., and Pastori, L. 1981, *Publ. Astron. Soc. Pacific*, **93**, 237.
Asplund, M., Grevesse, N., Sauval, A. J., and Scott, P. 2009, *Annu. Rev. Astron. Astrophys.*, **47**, 481.
Baade, W. 1956, *Publ. Astron. Soc. Pacific*, **68**, 5.
Baglin, A. 2003, *Adv. Space Res.*, **31**, 345.
Bailer-Jones, C. A. L. 2015, *Publ. Astron. Soc. Pacific*, **127**, 994.
Balona, L. A. 2018, *Mon. Not. Roy. Astron. Soc.*, **479**, 183.
Balona, L. A., and Nemec, J. M. 2012, *Mon. Not. Roy. Astron. Soc.*, **426**, 2413.
Baran, A. S., Koen, C., and Porkrzywka, B. 2014, *Mon. Not. Roy. Astron. Soc.*, **448**, L16.
Bedding, T. R., *et al.* 2020, *Nature*, **581**, 147.
Breger, M. 1979, *Publ. Astron. Soc. Pacific*, **91**, 5.
Breger, M. 1990, *Delta Scuti Newsl.*, **2**, 13.
Breger, M. 2000, *Baltic Astron.*, **9**, 149.

Bressan, A., Marigo, P., Girardi, L., Salasnich, B., Dal Cero, C., Rubele, S., and Nanni, A. 2012, *Mon. Not. Roy. Astron. Soc.*, **427**, 127.
Gaia Collaboration, *et al.* 2018, *Astron. Astrophys.*, **616A**, 1.
Chevalier, C. 1971, *Astron. Astrophys.*, **14**, 24.
Cox, J. P. 1963, *Astrophys. J.*, **138**, 487.
Drake, A. J., *et al.* 2009, *Astrophys. J.*, **696**, 870.
Eker, Z., *et al.* 2018, *Mon. Not. Roy. Astron. Soc.*, **479**, 5491.
Elst, E. W. 1978, *Inf. Bull. Var. Stars*, No. 1442, 1.
Flower, P. J. 1996, *Astrophys. J.*, **469**, 355.
Garg, A., *et al.* 2010, *Astron. J.*, **140**, 328.
Gilliland, R. L., *et al.* 2010, *Publ. Astron. Soc. Pacific*, **122**, 131.
Guzik, J. A. 2021, *Frontiers Astron. Space Sci.*, **8**, 653558 (doi: 10.3389/fspas.2021.653558).
Henden, A. A., Welch, D. L., Terrell, D., and Levine, S. E. 2009, *Bull. Amer. Astron. Soc.*, **41**, 669.
Henden, A. A., Terrell, D., Welch, D., and Smith, T. C. 2010, *Bull. Amer. Astron. Soc.*, **42**, 515.
Henden, A. A., Levine, S. E., Terrell, D., Smith, T. C., and Welch, D. L. 2011, *Bull. Amer. Astron. Soc.*, **43**, 2011.
Holdsworth, D. L., *et al.* 2014, *Mon. Not. Roy. Astron. Soc.*, **439**, 2078.
Hoffman, D. I., Harrison, T. E., and McNamara, B. J. 2009, *Astron. J.*, **138**, 466.
Jayasinghe, T., *et al.* 2021, *Mon. Not. Roy. Astron. Soc.*, **503**, 200.
Joshi, S., and Joshi, Y. C 2015, *J. Astrophys. Astron.*, **36**, 33.
Jurcsik, J., *et al.* 2005, *Astron. Astrophys.*, **430**, 1049.
Kukarkin, B. V., Parenago, P. P., Efremov, Yu. N., and Kholopov, P. N. 1951, *The Catalogue of the Stars of Suspected Variability*, Academy of Sciences, Moscow.
Laney, C. D., Joner, M., and Rodriguez, E. 2003, in *Interplay of Periodic, Cyclic and Stochastic Variability in Selected Areas of the H-R Diagram*, ed. C. Sterken, Astron. Soc. Pacific Conf. Ser. 292, Astronomical Society of the Pacific, San Francisco, 203.
Leavitt, H. S., and Pickering, E. C. 1912, *Circ. Harvard Coll. Obs.*, No. 173, 1.
Lee, Y.-H., Kim, S. S., Shin, J. Lee, J., and Jin, H. 2008, *Pub. Astron. Soc. Japan*, **60**, 551.
Lenz, P., and Breger, M. 2005, *Commun. Asteroseismology*, **146**, 53.
Lindegren, L., *et al.* 2016, *Astron. Astrophys.*, **595A**, 4.
Minor Planet Observer. 2010, MPO Software Suite (http://www.minorplanetobserver.com), BDW Publishing, Colorado Springs.
McNamara, D. H. 2000, in *Delta Scuti and Related Stars*, eds. M. Breger, M. Montgomery, Astron. Soc. Pacific Conf. Ser., 210, Astronomical Society of the Pacific, San Francisco, 373.
McNamara, D. H. 2011, *Astron. J.*, **142**, 110.
Nemec, J. M., Balona, L. A., Murphy, S. J., Kinemuchi, K., and Jeon, Y.-B. 2017, *Mon. Not. Roy. Astron. Soc.*, **466**, 1290.
Niu, J.-S., Fu, J.-N., and Zong, W.-K. 2013, *Res. Astron. Astrophys.*, **13**, 1181.
Niu, J.-S., *et al.* 2017, *Mon. Not. Roy. Astron. Soc.*, **467**, 3122.
Paunzen, E., and Vanmunster, T. 2016, *Astron. Nachr.*, **337**, 239.
Poretti, E. 2003a, *Astron. Astrophys.*, **409**, 1031.
Poretti, E. 2003b, in *Interplay of Periodic, Cyclic and Stochastic Variability in Selected Areas of the H-R Diagram*, ed. C. Sterken, ASP Conf. Ser. 292, Astronomical Society of the Pacific, San Francisco, 145.
Poro, A., *et al.* 2021, *Publ. Astron. Soc. Pacific*, **133**, 084201.
Qian, S.-B., Li, L.-J., He, J.-J., Zhang, J., Zhu, L.-Y., and Han, Z.-T. 2018, *Mon. Not. Roy. Astron. Soc.*, **475**, 478. [2018 not 2017]
Ricker, G. R., *et al.* 2015, *J. Astron. Telesc, Instrum. Syst.*, **1**, 014003.
Rodríguez E. and Breger M. 2001, *Astron. Astrophys.*, **366**, 178.
Schlafly, E. F., and Finkbeiner, D. P. 2011, *Astrophys. J.*, **737**, 103.
Schlegel, D. J., Finkbeiner, D. P., and Davis, M. 1998, *Astrophys. J.*, **500**, 525.
Schwarzenberg-Czerny, A. 1996, *Astrophys. J.*, **460L**, 107.
Serenelli, A., Scott, P., Villante, F. L., Vincent, A. C., Asplund, M., Basu, S., Grevesse, N., and Peña-Garay, C. 2016, *Mon. Not. Roy. Astron. Soc.*, **463**, 2.
Shappee, B. J., *et al.* 2014, *Astrophys. J.*, **788**, 48.
Skrutskie, M. F., *et al.* 2006, *Astron. J.*, **131**, 1163.
Smith, T. C., Henden, A. A., and Starkey, D. R. 2011, in *The Society for Astronomical Sciences 30th Annual Symposium on Telescope Science*, Society for Astronomical Sciences, Rancho Cucamonga, CA, 121.
Software Bisque. 2019, TheSkyX professional edition 10.5.0 (https://www.bisque.com).
Templeton, M. R., Samolyk, G., Dvorak, S., Poklar, R., Butterworth, N., and Gerner, H. 2009, *Publ. Astron. Soc. Pacific*, **121**, 1076.
Torres, G. 2010, *Astron. J.*, **140**, 1158.
Unsold, M. 2000, ImagesPlus Ver. 6.5 (http://www.mlunsold.com/ILOrdering.html).
Uytterhoeven K., *et al.* 2011, *Astron. Astrophys.*, **534A**, 125.
Vagnozzi, S. 2019, *Atoms*, **7**, 41.
Vanmunster, T. 2011, light curve and period analysis software, Peranso v.2.50 (https://www.cbabelgium.com/peranso).
von Steiger, R., and Zurbuchen, T. H. 2016, *Astrophys. J.*, **816**, 13.
Walker, G., *et al.* 2003, *Publ. Astron. Soc. Pacific*, **115**, 1023.
Wang, R., *et al.* 2019, *Pub. Astron. Soc. Pacific*, **131**, 024505.
Warner, B. D. 2007, *Minor Planet Bull.*, **34**, 113.
Watson, C., Henden, A. A., and Price, C. A. 2014, AAVSO International Variable Star Index VSX (Watson+, 2006–2014; https://www.aavso.org/vsx).
Wesselink, W. J. 1946, *Bull. Astron. Inst. Netherlands*, **10**, 91.
Wils, P., *et al.* 2011, *Inf. Bull. Var. Stars*, No. 5977, 1.
Wils, P., *et al.* 2012, *Inf. Bull. Var. Stars*, No. 6015, 1.
Wils, P., *et al.* 2013, *Inf. Bull. Var. Stars*, No. 6049, 1.
Wils, P., *et al.* 2014, *Inf. Bull. Var. Stars*, No. 6122, 1.
Wils, P., *et al.* 2015, *Inf. Bull. Var. Stars*, No. 6150, 1.
Woźniak, P. R., *et al.* 2004, *Astron. J.*, **127**, 2436.
Xiong, D. R., Deng, L., Zhang, C., and Wang, K. 2016, *Mon. Not. Roy. Astron. Soc.*, **457**, 3163.
Yang, T.-Z, Sun, X.-Y., Zuo, Z.-Y. and Liu, H.-W. 2021, *Astron. J.*, 161, 27.
Zacharias, N., *et al.* 2010, *Astron. J.*, **139**, 2184.
Zhao, G., Zhao, Y.-H., Chu, Y.-Q., Jing, Y.-P., and Deng, L.-C. 2012, *Res. Astron. Astrophys.*, **12**, 723.
Ziaali, E., Bedding, T. R., Murphy, S. J., Van Reeth, T., and Hey, D. R. 2019, *Mon. Not. Roy. Astron. Soc.*, **486**, 4348.